FlySmart - Automatic Take-Off and Landing of an EASA CS-23 Aircraft

Federico Pinchetti*, Johannes Stephan*, Alexander Joos† and Walter Fichter ‡
Institute of Flight Mechanics and Control, University of Stuttgart,
Pfaffenwaldring 27, D-70569 Stuttgart, Germany

September 9, 2016

This paper describes a low complexity controller framework for automatic landing and take-off for general aviation aircraft without using any ground based facilities. In addition an efficient on-board path planning algorithm that enables worldwide full automatic mission execution is presented. The lean implementation of the control laws allows to guide the aircraft in all configurations and within the whole flight envelope with a minimal amount of control modes to facilitate future certification. An entire flight including the take-off, a cruise section, a holding pattern, the approach with configuration changes and the landing sequence is demonstrated on a Diamond DA42.

1 Introduction

In recent years a growing interest in automation for small aircraft may be observed. New full authority fly-by-wire systems, e.g. [1, 2], have the potential to enable automatic operations even for EASA CS-23 aircraft. In contrast to large commercial aircraft (CS-25), these aircraft often use small airports without ground based facilities, which requires automation functionalities to run completely on-board. Such functionalities were designed in the LUFO IV.4 project FlySmart, which was carried out as a collaboration between Diamond Aircraft, Airbus Defence & Space, and University of Stuttgart (iFR - Institute of Flight Mechanics and Controls, ILS - Institute for Aircraft Systems).

Reducing complexity of flight control laws is a key aspect for safe and automatic operation of an aircraft along a full flight mission. Moreover, this approach can facilitate future certification efforts, as well as familiarization by the pilots, enhancing the possibility for a widespread adoption.

A framework, containing planning and control algorithms, is here introduced that is useful to conduct flight operations on a twin-engine CS-23 aircraft, from runway line-up, take-off, cruise flight, approach, till landing with full stop on the runway. All functions are developed to be executable on-board and to safely operate the aircraft in all phases of the mission. Therefore, the planning algorithms are aimed at providing valid and flyable flight paths with no geographical restriction. At the same time, the control algorithms strive to provide a guaranteed performance within the aircraft envelope and for all possible aircraft configurations. These challenges lead to a setup with spline based path definition, scheduled multi-input / multi-output controllers with anti-windup, and full authority over the aircraft configuration. The proposed solution can also tackle challenges brought by technical and hardware limitations, such as performing the final approach and landing phases using only on-board sensors. Computationally efficient controllers with minimal complexity are able to cope with this large variety of scenarios thanks to an extensive testing and robustification Monte-Carlo campaign. In addition, the presented framework can guarantee that all automation functions are executed safely and without interruption despite limited computational power available on-board.

Figure 1: *DA42 Used for Flight Tests.*

The framework has been demonstrated in a flight test campaign, employing a DA-42, registration OE-FMP, see Fig. 1. These flights took place in Wiener

*Ph.D. Student.
†Postdoc, Deputy head of the institute.
‡Professor, Head of the institute.

Neustadt (A) during the Summer 2015 and have led to several succesful automatic landings, the first of which on August 26th 2015. This was followed by a complete automatic mission, including take-off, performed on September 18th 2015.

The flight control laws' structure is illustrated in Sec. 2, with details about the various components given in Sec. 3-6. The design and verification process in preparation for the flight tests, and the flight test campaign itself, are presented in Sec. 7.

2 Flight Control Laws Structure

The realization of a low complexity implementation is achieved through the analysis of a standard flight mission and the design of the different controller components around specific sets of tasks. Such sets are partially derived from the information contained in the Pilot Operational Handbook checklists [3], and Standard Operating Procedures [4] provided by the manufacturer. This leads to the structure shown in Fig. 2.

Path Planner works on demand. Given a list of waypoints, it generates the trajectory to be flown, and sends it to the mananger and the guidance functions. It also generates a reference trajectory for the final approach substitutive for an ILS glideslope.

Flight Control Manager (FCM) tracks which phase of the mission is being/to be performed, and sends this information to the guidance. It also deals with the discrete configuration changes, and the activation of special controls (brakes), shown as a dashed line in Fig. 2.

Guidance is designed around the aircraft kinematic behaviour, and handles changes in control objectives (see Tab. 1). It computes the reference values for the low level control loops.

Low Level Control (LLC) deals with the aircraft dynamics, and differentiates only between airborne and on ground, minimizing its complexity.

Focusing each component on a limited number of tasks allows high functional reusability and a reduction of the overall complexity. This led to a number of beneficial results that will be explored in Sec. 3-6, together with a detailed description of the four components.

3 Path Planner

The path planner is tasked with generating a flyable reference trajectory given a list of waypoints, similarly to what a pilot would do during pre-flight operations. The waypoints might be generated by an external path finding algorithm or may be assigned manually by the pilot, and the planner must not differentiate. This has led to the definition of a flexible and globally valid interface. Within said interface, the waypoints are defined as a location in the WGS84 frame. In addition, they are charaterized by the desired airspeed at the given location, and the phase of flight they belong to.

To minimize the complexity of the later control stages, the planner has to ensure flyability of the planned reference trajectory. In fact, by providing a flyable trajectory, the path planner allows the guidance and LLC to be designed around their given objectives, without adding any unnecessary complications. The flyability of the reference trajectory is guaranteed by taking into account the kinematic and dynamic limits of the aircraft, provided through a separate input. This guarantees that the planner is completely aircraft-independent, while at the same time it generates a safe path for the specific aircraft in use. In particular, the interface contains information about the range, limits on velocity, descent and climb rates, as well as maximum attitude angles and rates. On this basis, the planner is able to find a reference spatial path through a generalized 3D Dubins algorithm. This path is then augmented and a 4D trajectory is generated by adding a velocity profile to the 3D path. In a succesive stage, the planner approximates the trajectory with algebraic splines to obtain a homogeneous trajectory description. In this way, a single control algorithm is sufficient to track the displacement of the position and velocity. As described in Sec. 5 and 6, this approach enables a simplified closed loop control structure.

To ensure flexibility and to avoid restrictions on the location of the flights, the spatial path is defined in a UTM-based cartesian reference frame. This also allows the generation of long range flight plans without loss of precision, suited for take-off and landing phases. To reduce the occurrence of numerical precision glitches, not only the standard UTM zones have been employed (one each 6° of longitude), but also internally-defined intermediate zones. This doubled the number of available zones, one each 3° of longitude, leading to significant and useful overlapping between adjacent zones. South to north, instead, each zone has been subdivided in 20 areas, limiting the size to $1000km$. The overall result from this methodology is that northing and easting UTM coordinates never exceed 10^6m, which leads, in the worst case, to an accuracy error of $10^{-1}m$ in single floating point precision, deemed satisfactory to perform precision approaches and landings.

In addition, the holding patterns are planned with standard entries (direct, parallel and teardrop) to facilitate integration in a supervised airspace. The final approach is instead planned as a descent with a 3°

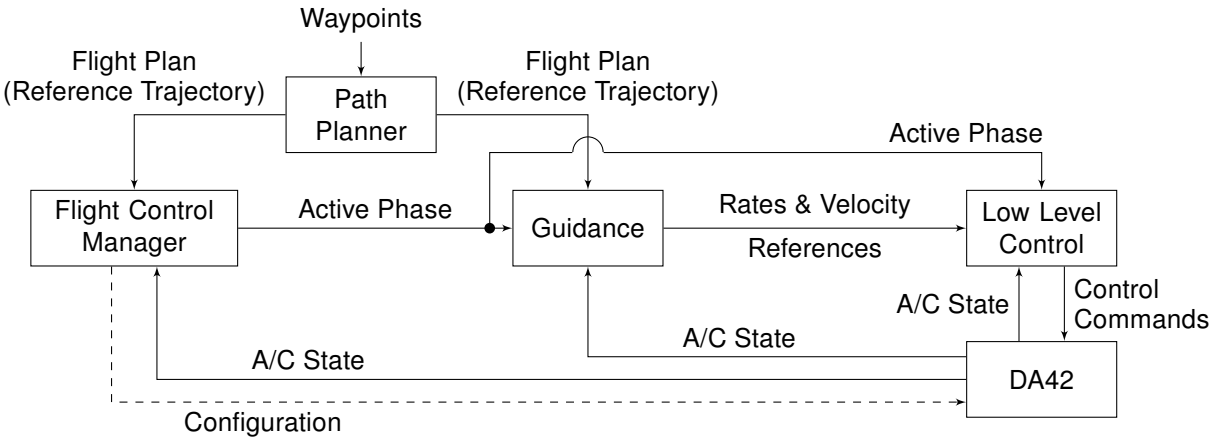

Figure 2: *Flight Control Laws Structure.*

slope with respect to the runway, to simulate the presence of an ILS glideslope.

An example of a planned mission is presented in Fig. 3 and Fig. 4. The mission is to the east of the Wiener Neustadt Ost (ICAO code: LOAN), also to respect the airspace restrictions in place in the area. Special markers highlight where configuration changes are triggered by the FCM. The shaded area in Fig. 4 illustrates the ground elevation.

4 Flight Control Manager

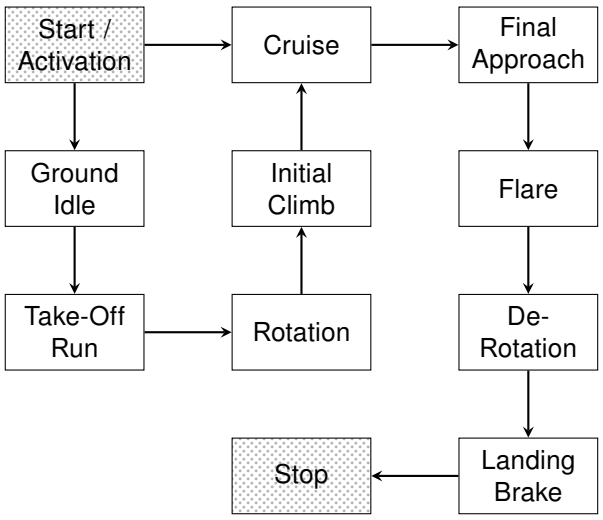

Figure 5: *Flight Control Manager State Machine.*

The FCM supports the pilot or operator in supervising the systems, and mainly acts as an overseer of the guidance and LLC blocks. Its primary task is to keep track of the phase of flight being performed, and to optionally interact with the operator (or possibly an automated ATC interface) if ATC clearances are desired. This is used to prevent unsafe activation of the system, as well as rendering operative only those control loops that are required. In addition, it takes care of safely perform configuration changes (flap and gear extension/retraction) at pre-determined locations along the flight path. This is obtained through the use of a simple state-machine, shown in Fig. 5. The actions performed in each of the states can be briefly summarized as follows.

Start/Activation is a stand-by state used while determining if it is safe to transition to a state of active control.

Ground Idle is a state in which the aircraft is standing still on ground, awaiting take-off clearance.

Take-off run is characterized by the aircraft still on the ground; it is characterized by a different dynamic system from flight conditions, the lack of aileron and elevator activity, and the throttle is open-loop controlled.

Rotation is the transition between dynamic systems; pitch attitude and rate are limited; the throttle is still open-loop.

Initial climb contains the first changes of configuration; pitch attitude is used to control speed; the throttle is still in open-loop.

Cruise covers most of the flight; clean configuration; 4D path following.

Final approach includes changes in configuration; there is no change in control objectives.

Flare denotes the presence of the aerodynamic ground effect; reduced bank limits; sink rate must be controlled.

De-rotation is the other transition between dynamic systems; the main gear is on ground; limited/no banking authority; pitch rate is limited while lowering the nose; throttle is cut-off.

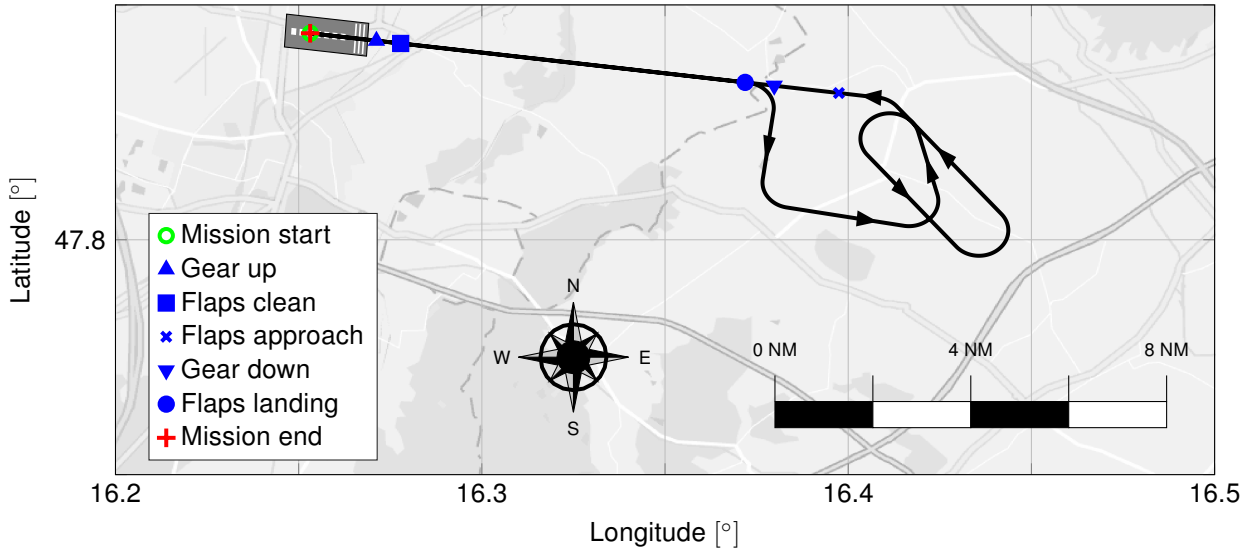

Figure 3: *Automatic Landing Mission - Reference Ground Track.*

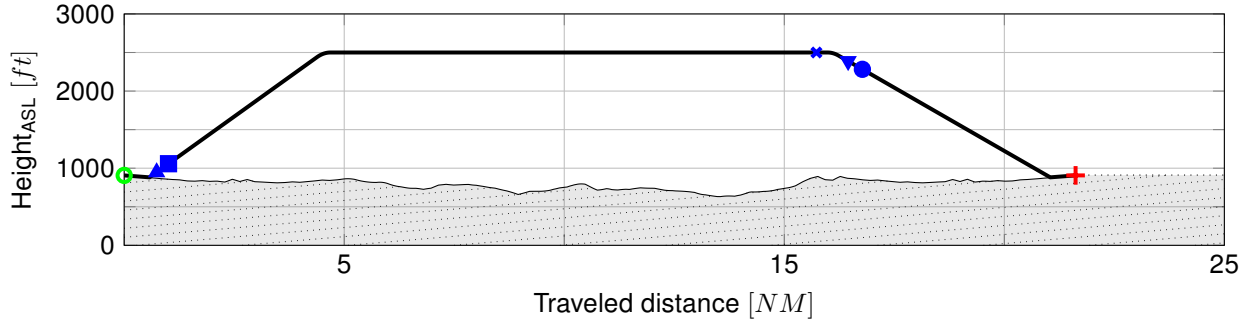

Figure 4: *Automatic Landing Mission - Reference Altitude.*

Landing brake is characterized by the aircraft on the ground; same dynamic system as take-off; there is no elevator activity; throttle/engine off; brake activation.

Stop is reached once the aircraft completely halt after the landing brake, and the system is deactivated determining a successful mission completion.

The activation of the system prompts the FCM to check the status of the aircraft. The FCM allows a transition to an automated control mode only if the aircraft is standing still on ground (indicating a preflight condition) or is in flight in clean configuration (indicating cruise). Other transitions from the activation state are not allowed for safety reasons. The remaining transitions between the states are dictated by the measured aircraft state together with the planned path, or by pilots inputs corresponding to ATC clearances (permission to take-off and clearance to land). This last point contributes to making the system interoperable with a possible (semi-)automated ATC controller.

Having merged all transition rules related to the decision-making into the FCM, the guidance and LLC are implemented as generic collections of computationally efficient control functions. As described in Sec. 5 and 6 these are combined into specific flight control laws suited to the requirements of the actual flight phase, given by the FCM, without requiring a specific set of controllers to be designed for each different phase. Therefore, decoupling the decision-making and the basic control functions supports simple and efficient algorithms.

5 Guidance

The guidance ensures that the planned trajectory, which consists of a continuous sequence of reference locations and velocities, is followed in an accurate and precise manner. As an output, it delivers references for the body angular rates as well as the flight velocity to the inner loops, see Fig. 2. As can be seen from Tab. 1, the control strategy of the guidance is adapted to different kinematic constraints and mission objec-

		Lateral control		Longitudinal control	
		Error Value	Control Variable	Error Value	Control Variable
Guidance	Ground	Lat. deviation	Yaw Rate	-	-
		-	-	-	-
	Rotation & De-Rotation	Lat. deviation	Yaw Rate	Pitch attitude	Pitch rate
		-	-	-	-
	Climb	Lat. deviation	Roll Rate	Velocity deviation	Pitch rate
		Sideslip	Yaw rate	-	-
	Cruise & Approach	Lat. deviation	Roll Rate	Vert. deviation	Pitch rate
		Sideslip	Yaw rate	Velocity reference	
	Flare	Lat. deviation	Roll Rate	Pitch attitude	Pitch rate
		Sideslip	Yaw rate	Sink rate	Velocity ref. eq.
Low Level Control	Ground	Yaw Rate	Nose Wheel	-	-
		-	-	-	-
	Flight	Roll Rate	Aileron cmd	Pitch rate	Elevator cmd
		Yaw rate	Rudder cmd	Velocity ref	Throttle cmd

Table 1: *Guidance and Low Level Control Interfaces.*

tives depending on the active phase. In addition, it can be noted that the number of different guidance loops necessary to drive the aircraft along the complete flight mission is reduced with respect to the number of states present in the FCM.

During the take-off run, a reference yaw rate is used to control the lateral displacement, whereas the roll- and pitch-rates are constrained by the ground and thus do not need to be considered. While the rotation phase is active, the pitch attitude is controlled via a reference pitch rate. For all ground based operations, a predetermined thrust is applied.

Once the take-off sequence is finished, the structure of the lateral controller remains for all airborne operations: the lateral displacement of the position is tracked to zero by a cascade control system via a reference roll rate. Furthermore, the sideslip angle is minimized by setting a reference yaw rate. A major benefit of this unification of the control objective is a reduced complexity of the algorithm, which results in less implementation and verification effort.

In contrast, different control strategies apply in the longitudinal motion during the initial climb phase, the cruise and approach phase, and the flare. In the former, the reference pitch rate is used to control the velocity and the thrust is set open-loop. For both, cruise and approach, a cascaded control loop delivers a reference pitch rate in order to minimize the vertical displacement of the position, while the reference velocity comes directly from the planned trajectory. At the end of the final approach, the system performs a flare, which requires another change in the longitudinal control objective. During this phase, the pitch attitude is tracked by setting a reference pitch rate. Simultaneously the sink rate is controlled via a reference velocity.

In order to perform the de-rotation, the pitch attitude is again controlled with a reference pitch rate. Back on ground again, the landing run is performed similarly to the take-off run, where only a reference yaw rate is applied in order to track the lateral displacement of the position.

All guidance loops are designed as single-input and single-output (SISO) feedback loops. The control structure is a cascade of proportional-integral-derivative (PID) subsets. The various gains are designed using standard frequency domain methods. To this end, a set of design models was defined, representing the kinematics of the aircraft.

In order to optimize the tracking accuracy, the guidance loops are assisted by feed-forward signals, which correspond to the reference spatial and velocity profiles. Based on the assumption of symmetric flight with zero wind, reference values for the path angles, the bank angle, and the body rates are obtained using differential flatness properties of the planned trajectory, which involves the splines and their derivatives.

6 Low Level Control

The purpose of the LLC is to adjust the dynamics of the fast rigid body motion and by the same time track given references for the body angular rates as well as the flight velocity. To this end it distinguishes only between two dynamical systems: airborne and ground operations, which enables an efficient and lean implementation.

When in flight, the rate tracker generates commands for the deflection of the aerodynamic surfaces aileron, rudder, and elevator. The monolithic loop is designed as a multi-input multi-output (MIMO) channel PI controller based on a full state-feedback. The design model involves the fast period in the vertical motion and the dutch roll and the roll dynamics in the lateral motion, which all heavily depend on the dynamic pressure. The gains are therefore scheduled over the flight velocity in order to achieve robust stability and performance within the whole flight envelope. In the event of actuator saturation, the nominal loop is assisted by a static MIMO anti-windup augmentation, which feeds the saturation errors back into the controller. The gain synthesis for both, the nominal controller as well as the anti-windup augmentation, is carried out using state space approaches such as the linear-quadratic regulator (LQR) and modern LMI based methods, see [5, 6]. Since the aerodynamic properties of the aircraft change substantially in the event of a gear extension or a modification of the flap setting, a separate set of gains is applied for each configuration.

In addition, the LLC controls the thrust via the throttle command given a reference velocity. The velocity controller implements a PI structure with frequency based filters to achieve smooth behavior in normal conditions and fast reactions in critical situations such as longitudinal gusts. The performance is further improved by applying a feed-forward based on the path angle and the target velocity. To this end, a modeling of the aerodynamic resistance as well as the propulsion unit is used. As described in Sec. 4 and 5, the thrust is set open loop in certain mission phases. Therefore the thrust control loop is occasionally deactivated.

On ground, the LLC is used to track the reference yaw rate by setting the steering angle deflection of the front wheel, which is mechanically linked to the rudder.

7 Flight Test Campaign

In Autumn 2015, the functionality of the controller framework was demonstrated as part of a flight test campaign, which took place at Wiener Neustadt East Airport (LOAN), Austria. Within this work, a Diamond Aircraft DA-42 Twin Star, which was equipped with a fly-by-wire platform (see [7, 8]), served as the experimental aircraft. The DA-42 is a light, low wing, utility and trainer aircraft, which is developed and produced by Austrian manufacturer Diamond Aircraft Industries, see Fig. 1. It is driven by synchronous rotating twin propellers, which are powered by two TAE 125-01 Centurion 1.7 diesel combustion engines. The aircraft seats up to four people while offering a flight range of more than $1000\,NM$, a ceiling of $18000\,ft$ and a maximum speed of $192\,Kts$. The DA-42 is designed as a monoplane, largely made of composite materials and is fitted with an electric flap system and a retractable tricycle landing gear, see [9].

The preflight testing included a series of comprehensive lab tests, which are summarized in Sec. 7.1. Subsequently, several flight tests were performed, leading to a successful demonstration of the ATOL capability. Flight data is presented in Sec. 7.2.

7.1 Flight Test Preparation

Preemptively to the first automatic flights, the controller was extensively tested with a variety of methods to evaluate and verify the robustness and performance of the control laws, as well as the correctness of the code.

Analytical investigation were applied in order to investigate the stability and dynamic behavior of the system under varying flight conditions. As an example, Lyapunov's indirect method was applied on the closed loop system for linearization points within the whole flight envelope. Fig. 6 shows the poles of the pitch rate controller in the vertical axis. The conjugated complex poles relate to the controlled short period whereas the real pole is associated to the controller integrator. As can be seen, the system dynamics vary between different configurations.

Software in the Loop simulations were necessary to guaranty the robustness of the low complexity control structures within the whole flight envelope and different aircraft configurations even in the presence of model uncertainties.

Using a computer cluster, several thousand simulation runs under varying conditions were performed and automatically evaluated for safety and performance of the flight. The different runs were configured based on stochastic distributions for the aircraft weight and balance, crucial aerodynamic coefficients and the wind condition. In order to assess the success and performance of each run, numerical criteria such as permitted touchdown area, attitude, sink rate, and loads on the gear, were obtained from the

Certification Specification for All Weather Operations [10]. Those were reparametrized based on the Pilot Operational Handbook checklists [3], and Standard Operating Procedures [4] where needed.

In Fig. 7 a small extract from the simulation results is presented. The plot shows the altitude displacement over time for the initial part of the approach, which includes the gear extension and a change of the flap setting. Between the presented runs the aerodynamic parameters of the pitch dynamic differ up to $\pm 70\%$ from the nominal model.

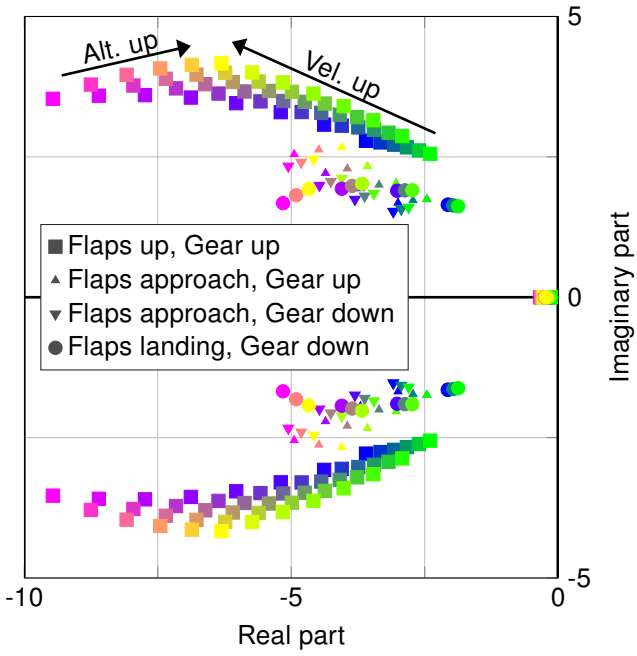

Figure 6: *Indirect Lyapunov Method.*

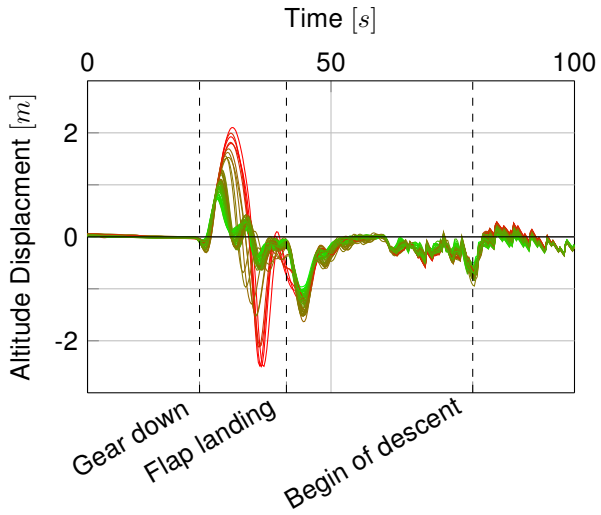

Figure 7: *Monte Carlo Study, Aerodyn. Parameters* $\pm 70\%$.

Hardware in the Loop runs were used to integrate the algorithms into the system and improve the computational efficiency on the target hardware, as well as to test the human-machine interface.

Altogether the lab tests generated high confidence in the system and laid the basis for a very efficient flight test campaign.

7.2 Flight Test Execution

Each functionality described in the previous Sec. 3-6 has been tested and demonstrated in separate flight scenarios, which progressively led towards a full mission. As a first step, several high-altitude flights were conducted to verify the lab test results under operating conditions. The cruise control has been directly and throughly tested in a series of dedicated tests including climbs, descends, velocity changes, coordinated turns, and changes of the configuration.

Subsequently, a number of simulated flares were executed at high altitudes, to familiarize the pilots with the implemented landing procedure. To demonstrate the functionality of the system in conditions near to the ground and under the influence of the ground effect, the test altitude was then lowered step by step. The capability of the centerline keeping was verified simultaneously in dedicated ground tests. These preparatory steps resulted in a series of automatic landing tests in August 2015. On September 17^{th}, 2015 a complete test mission including an automatic take-off was successfully accomplished at the first attempt. The ground track of this mission is shown in Fig. 3, with the corresponding altitude profile presented in Fig. 4. After powering up the system at the end of the runway, the pilots activated the flight control system, which was followed by the automatic take-off run. Past to the initial climb, the DA-42 performed a cruise section, a holding pattern, and the approach, including various configuration changes. The subsequent flare led to a successful landing, which was concluded by the roll-out until a full stop was reach. For demonstration purposes, system interactions with the pilots were active within the scope of this test, enabling consideration of ATC clearances.

In the following, flight data from this first fully automated mission is presented. Fig. 8 shows the ground velocity and altitude over time during the automatic take-off. As can be seen, an acceleration phase is performed for about $28\,sec$ before the rotation speed of $85\,kts$ is reached. The clearance altitude of $50\,ft$ is passed another $3\,sec$ later. During the initial climb, the objective is to track a reference velocity of $90\,kts$ using a commanded pitch rate, see Fig. 9. In addition, the lateral displacement of the aircraft is controlled via a roll rate. For safety reasons, the bank authority is limited during the rotation phase, leading to an overall

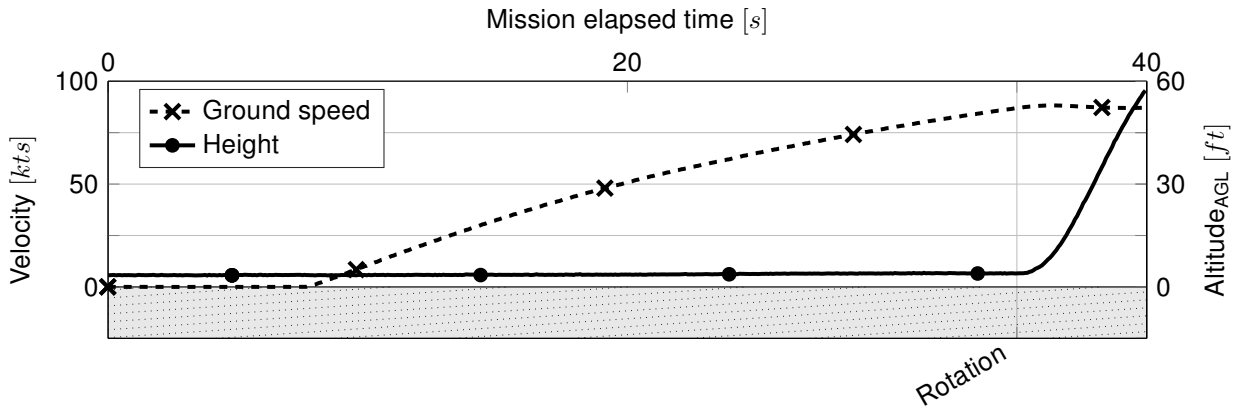

Figure 8: *Take-Off Run.*

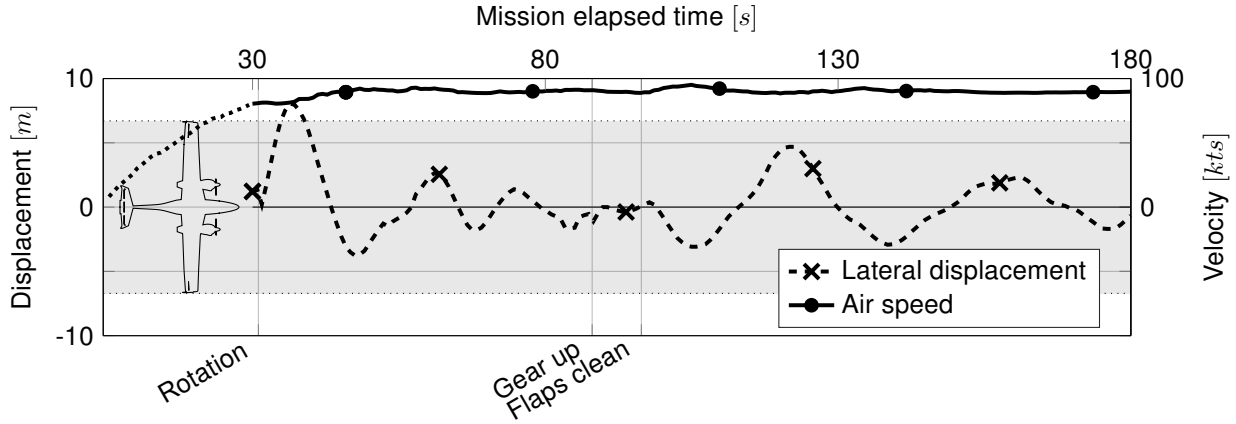

Figure 9: *Initial Climb.*

peak in the position error of approximately one wing span around $35\,sec$. For the last part of the cruise as well as the approach, the displacements of the position over time are shown in Fig. 10. The plot underlines the ability of the control system to maintain high spatial accuracy even in turning flight ($550 - 590\,sec$) and for different configuration changes ($600 - 660\,sec$), allowing a very precise final approach, despite a set of gusts occurring around $750 - 830\,sec$. The flare performance is depicted in Fig. 11 through the pitch attitude and the altitude above ground over time. After the flare is triggered at $842\,sec$, the pitch angle is increased over time to slow down the sink rate. Shortly above ground, the pitch rate reaches $4°$, which guaranties a collision-free touchdown of the main gear. The de-rotation at $851\,sec$ ensures a firm ground contact of the nose wheel as well, which provides the basis for reliable steering and thus enables the centerline keeping. The subsequent braking leads to a full stop again, which completes the first fully automated flight.

8 Conclusion

The simple and efficient flight control structure, and thorough pre-flight verification activities have contributed to overcome the natural skepticism of the test pilots, that originally saw this system as a possible competitor, as well as an unfamiliar companion in the cockpit. Through the performance of the various flight test stages, the pilots came to appreciate the system and its capabilities, giving an optimistic outlook to the possibility of making these systems more common and accepted.

References

[1] Maxim Lamp and Robert Luckner. Automatic landing of a high-aspect-ratio aircraft without using the thrust. In *Advances in Aerospace Guidance, Navigation and Control*, pages 549–567. Springer, 2015.

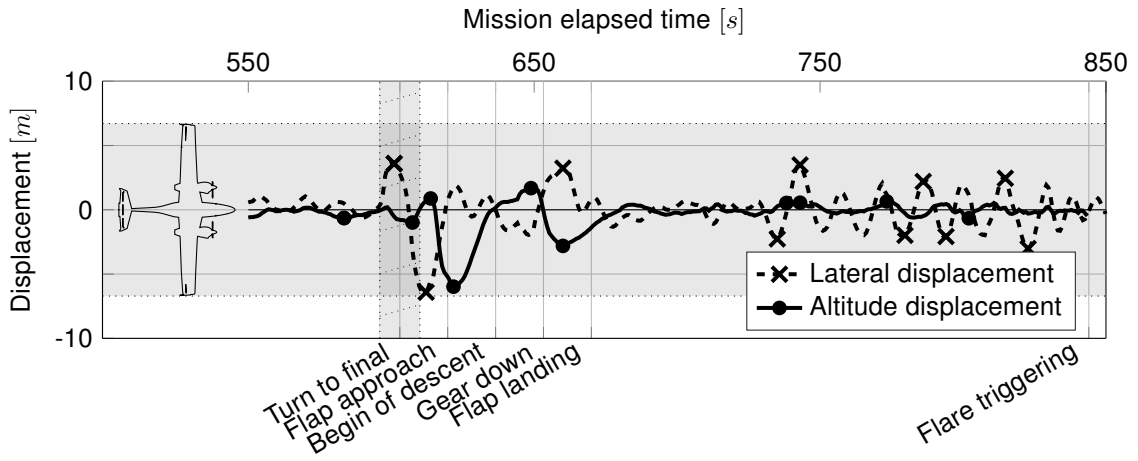

Figure 10: *Cruise and Approach.*

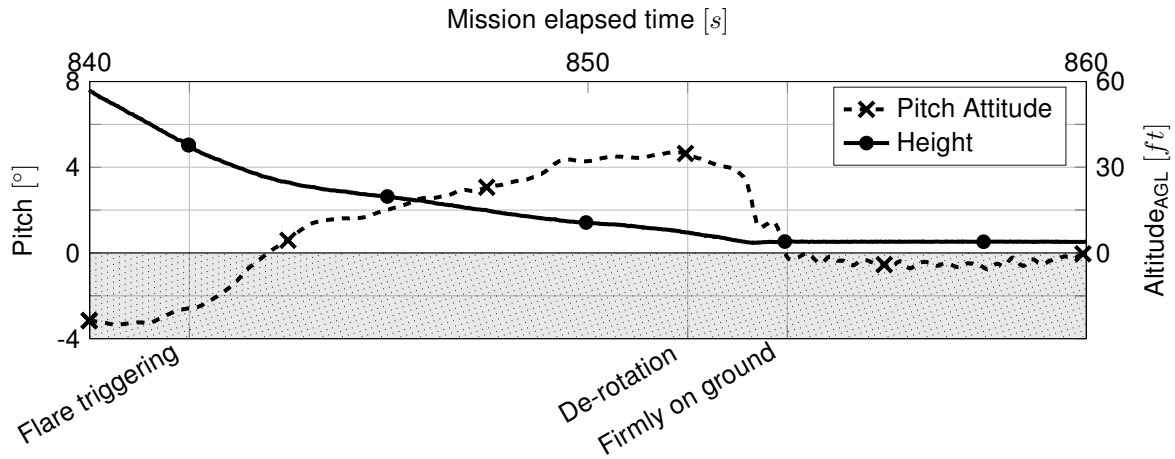

Figure 11: *Flare.*

[2] Oliver Marquardt, Marc Riedlinger, Reza Ahmadi, and Reinhard Reichel. An adaptive middleware approach for fault-tolerant avionic systems. In *Aerospace Conference, 2015 IEEE*, pages 1–8. IEEE, 2015.

[3] Diamond Aircraft Industries. *Airplane Flight Manual DA42*. Diamond Aircraft Industries, 2004.

[4] Diamond Executive Flugschule. *DA42 standard operating procedures*, 2011.

[5] Zlatko Emedi and Alireza Karimi. Robust fixed-order discrete-time lpv controller design. *IFAC Proceedings Volumes*, 47(3):6914–6919, 2014.

[6] Arief Syaichu-Rohman and Richard H Middleton. Anti-windup schemes for discrete time systems: An lmi-based design. In *Control Conference, 2004. 5th Asian*, volume 1, pages 554–561. IEEE, 2004.

[7] Sebastian Polenz. *Generisches Sensor Redundanz Management für eine flexible, fehlertolerante Plattform*. Verlag Dr. Hut, 2013.

[8] Simon Görke, Rolf Riebeling, Florian Kraus, and Reinhard Reichel. Flexible platform approach for fly-by-wire systems. In *2013 IEEE/AIAA 32nd Digital Avionics Systems Conference (DASC)*, pages 2C5–1. IEEE, 2013.

[9] European Aviation Safety Agency. Easa type-certificate data sheet - da 42. volume 22, 2013.

[10] JC Wanner. Certification specifications for all weather operation, cs-awo. 2003.